

# Corrosion evaluation for steel 316L with oxide coatings Ti-Zr-Si deposited by sol gel

Karla Dayana Guerrero\*, Erika Lorena Medina\*, Néstor Giovanni Yomayuzá\*, Jhon Jairo Olaya-Flórez\*, Jorge Hernando Bautista-Ruiz\* and Carlos Alberto Guerrero-Fajardo\*\*

\* Mechanical Engineering Department, Universidad Nacional de Colombia

\*\* Chemistry Department, Universidad Nacional de Colombia

**Abstract**-Stainless steels are widely used in engineering activities due to its chemical and mechanical features that offer high corrosion resistance as well as a good relationship of mechanical strength, resistance to high temperatures. Several methods known in surface engineering can be used to optimize the properties against corrosion of this kind material. The coating adhesion mechanism is a chemical anchor, which can provide the necessary protection for steel and used in various industrial and construction applications. This work displays the evaluation of performance against corrosion at high temperatures of a steel 316L with oxide coatings Ti-Zr-Si deposited by sol gel, which allows obtaining a ceramic system, deposited and analyzed with a mono, bi and tri-layer architecture presenting the results for each of them, carried out an analysis of loss of weight, chemical composition by energy dispersive X-ray (EDS) and scanning electron microscopy (SEM). The coating tri-layer 10/70/20 showed better corrosion protection at high temperatures, less cracking and roughness changes.

**Keywords:** Coating Si-Ti-Zr, corrosion resistance, Sol-Gel, Stainless Steel.

## I. INTRODUCTION

The process of corrosion in materials have always been tried to avoid in the whole industry, as this can potentially cause great economic losses, a widely used method for this is the application of coatings on surfaces which could be exposed to the environment or other important factors that may have an influence on them, these coatings have the function of reducing deterioration, these coatings are made from both synthetic and natural compounds that when applied to a surface offer protection of the environment [1, 2, 3]. Corrosion is an electrochemical process therefore an increase in the surface of the material will function as protection [4].

One method used for depositing the coatings on the substrate is the method of sol-gel, this is a chemical process that is within colloid chemistry, this method has some advantages over traditional methods such as: potential to produce compounds of high purity, with homogeneity at the atomic scale, its ability to greatly reduce temperatures and treatment time required to form the final product and its potential for good control of particle size [5, 6]. The sols are colloidal dispersions with a liquid with diameters between 1 and 100 nm. Once the sol form solid particles begin to form aggregates which are hydrolyzed and

polymerize by condensation, forming lattices where the gel molecules are encapsulated, forming a more viscous structure known as gel [7, 8, 9]. The traditional sol gel method has as starting reagents alkoxides; but because of its high cost and high reactivity with water is complicated handling because they react with the moisture present in the air and furthermore its large-scale production is limited [10, 11].

To study the behavior of a material to oxidation we can divide it into two categories, isothermal oxidation tests (constant temperature) and cyclic oxidation. Many applications of these studies require heating and cooling cycles, reason for which it is appropriate that the materials allow the slow formation of oxides to withstand mechanical damage during cycles. Cooling cycles lead to an increase in compressional efforts, this occurs because the thermal expansion coefficients of the substrates are higher by 30-50% than oxides. This may result in cracking of the oxide layers, delamination and detachment of the material. These are some of the reasons why the cyclic tests are more severe than isothermal oxidation by this test is possible to evaluate the lifetime of the oxide layer, estimate the adherence of the oxide layer and its resistance to cracking and spalling [12].

In this paper a coating of Ti-Si-Zr type is studied and as antecedents different studies have been performed on this topic using stainless steels with coatings of  $\text{SiO}_2\text{-ZrO}_2$  [5], where no satisfactory results were obtained due to the thickness of the coating layers and speed densified. In 2011, coatings were made with  $\text{SiO}_2\text{-TiO}_2\text{-ZrO}_2$ , experiment showed good anticorrosion results demonstrating the ability of this compound in sol-gel coating by decreasing the corrosion rate by 89% and was observed that the layer exhibited good adhesion to the substrate (steel 1020) being this an optimal anticorrosive coating [13].

## II. METHODOLOGY

### A. Coating preparation

The process developed for the formation of the sols was as follows: First, two separate solutions were prepared, the first one contained half the volume of ethanol solvent, (EtOH), the total volume of complexing (2,4-pentanedione), the total volume of precursor titanium, titanium tetrabutoxide  $[\text{Ti}(\text{OBU})_4]$  and the total volume of the precursor of zirconium, zirconium tetrabutoxide  $[\text{Zr}(\text{OC}_3\text{H}_7)_4]$ . The second one contained half volume of ethanol, the total volume of silicon precursor, tetraethylorthosilicate  $[\text{Si}(\text{OC}_2\text{H}_5)_4]$  and half the volume of

water. The two solutions were mixed considering that alcohol plays the role of solvent and water initiates the process of pre-hydrolysis of  $\text{Si}(\text{OC}_2\text{H}_5)_4$ . To get a good miscibility of the precursors and therefore good homogenization of the solutions, these were mixed using stirring at 400 rpm, temperature of 15 °C, 546 mm Hg pressure and a time of two hours. The substrates used for depositing multicomponent system Si/Ti/Zr: 10/70/20 were steel sheets AISI / SAE316L of dimensions 2 cm x 2 cm x 0.4 cm, polished until metallographic brightness, degreased for 15 minutes using ultrasound equipment with acetone and dried with hot air. The next step was to form films by dip-coating, at a rate of extraction 13,2cm/min. Sintering of the films was conducted at a heating rate of 1 °C/min permitting removal in a controlled manner, the organic component of the films. This process seeks to avoid pore formation and that the difference in thermal expansion present in the metal-coating interface, not favoring cracking coatings made.

### B. Heating program

The heating program used was the following:

Tri-layers: It starts with room temperature and is raised to 50 °C. There is maintained for one hour and is then carried to 100 °C for half an hour. For each of the deposited layers after sintering process are carried at room temperature to the cooling rate of the furnace.

### C. Testing Material Protection

For testing protection coating at high temperatures, the coated samples were taken to an electric furnace and subjected to 120 cycles of heating up to 600 °C for 60 minutes and cooling to room temperature for 60 minutes. At the end of the programmed number of cycles, we proceeded to determine the weight of the sample in an analytical balance and then be compared with the weight initially taken.

### D. Structural analysis

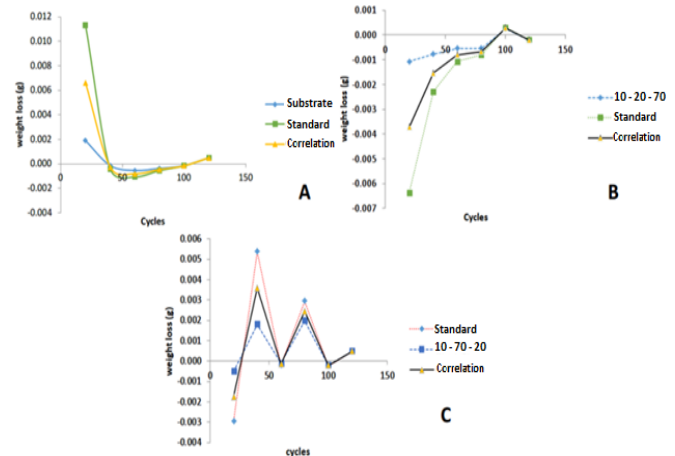
The crystal structure of the films is analyzed in a X-ray diffractometer (XRD) of polycrystalline samples, model Xpert brand Panalytical with Cu K radiation ( $\lambda = 1.5406\text{\AA}$ ) and an instrument resolution of 0.02 ° in configuration 2 $\theta$ . And analysis of energy dispersive X-ray (EDS) were also performed to determine the elements present on the surface of the coatings. These analyzes were performed in a scanning electron microscope (SEM) Tescan vega3 with probe EDS Bruker brand to an energy of 15 keV.

## III. DISCUSSION AND RESULTS

### A. Gravimetric analysis

In Figure 1A, we display the results of weight loss for the samples in the corrosion test for high temperature. Calculations mass exchange have been performed according to ASTM G1 standard, tests were performed for different layer thicknesses of coating with cycles at 600 °C and a duration of 2 hours, including one hour of heating and one hour cooling.

It is evident that during the first few cycles the sample begins to generate a quick oxide layer, thereby generating a weight gain, as they go cycles we see that the material begins to lose weight by a loosening in the oxide layer until the 60 cycles, then turns to observe weight gain that verifies the generation of oxides on the surface of the sample, this behavior will be used as a guide to analyze the response of the coatings.



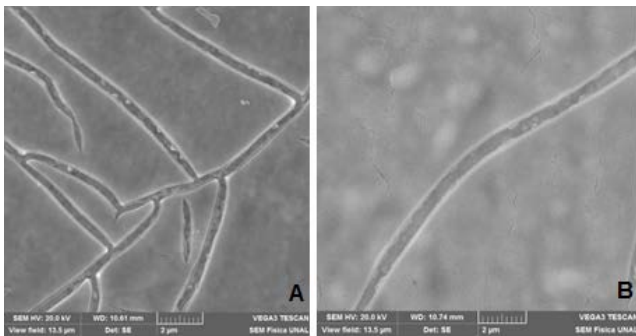
Source: Authors, 2016

Figure 1 Results weight loss analysis. A: Analysis weight loss substrate, B: Results for the analysis of weight loss of coating 10/20/70, C: Results for the analysis of weight loss of coating 10/70/20.

Analyzing the coating having composition 10/20/70 (Figure 1B) showed that during the first 20 cycles there is a weight loss, this is due to evaporation of the moisture contained in the coating and once it has reached 20 cycles, the weight begins to increase by suggesting oxide formation that cover and protect the material. Looking the coating with a 10/70/20 composition (Figure 1C), we can say that during the first 20 cycles also a weight loss is generated, suggesting that this is caused by the same reasons as the sample with a 10/20/70 composition but for this sample the generation of oxides is more fluctuating, suggesting a production and loosening of cyclic oxides may be caused by residues of the coating on the surface.

### B. SEM and EDS analysis

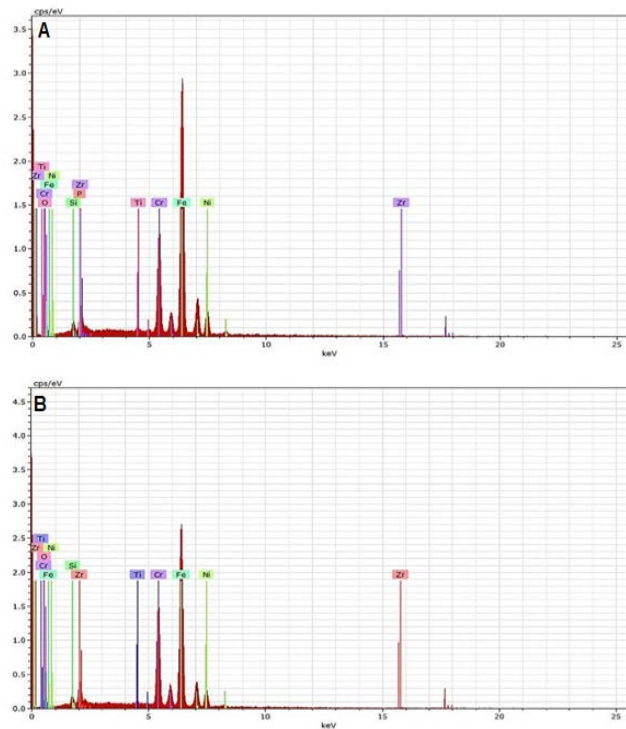
SEM analysis shows that for coating 10/20/70 (Figure 2) cracking is presented, thus explaining the behavior of the material weight, this suggests a difference between the coefficients of thermal expansion, being greater the base material and generating with expansions and contractions that produce the coating cracking generating a non-ideal behavior as corrosion protection at high temperatures, crystal formation can be assumed.



Source: Authors, 2016

Figure 2 Scanning electron microscopy A) SEM analysis Tri-layer 10/20/70 20 cycles 2 microns 20 keV; B) SEM analysis Tri-layer 10/20/70 120 cycles 2 microns 20 keV.

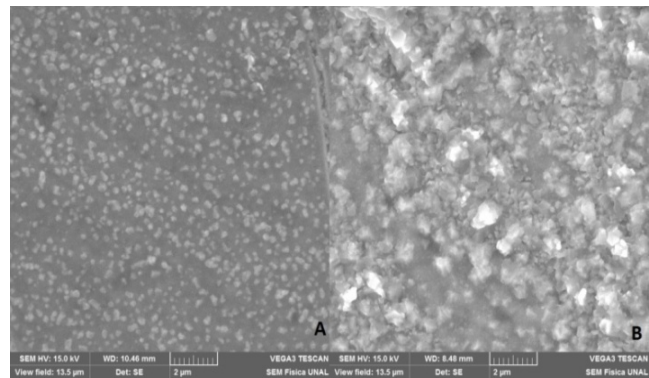
By EDS analysis (Figure 3) the coating 10/20/70 at 20 cycles having an approximate composition of FeO: 58.13% Cr2O3: 15.80%, NiO: 7.91% P2O5: 0.00%, SiO2: 2.39% and at 120 cycles have a composition FeO: 52.61% Cr2O3: 21.10%, NiO: 6.35% P2O5: 0.00%, SiO2: 2.06%.



Source: Authors, 2016

Figure 3 EDS analysis tri-layer 10/20/70 a) 20 cycles b) 120 cycles

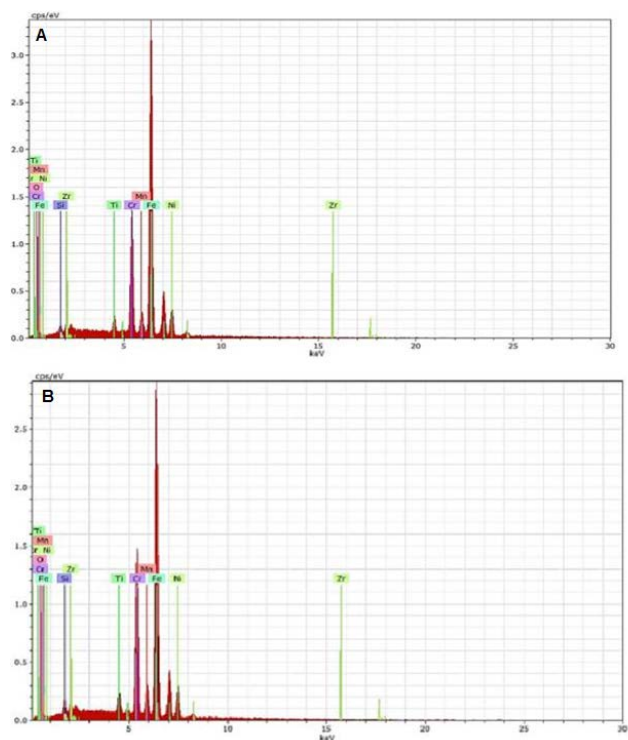
For the 10/70/20 composition, it can be observed the formation of a crystalline structure (Figure 4), suggesting a change in the structure of the coating, as it increases cycles can be observed by microphotographs that this has a structure amorphous, and that as the cycles increase is presented more clearly grain structure.



Source: Authors, 2016

Figure4 Scanning electron microscopy A) SEM analysis Tri-layer 10/70/20 at 20 cycles 2 microns 20 keV; B) SEM analysis Tri-layer 10/70/20 at 120 cycles 2 microns 20 keV

EDS results (Figure 5) for the composition of 10/70/20 at 20 cycles can be observed an approximate composition: FeO: 60.65%, Cr2O3: 15.10%, NiO: 6.32% P2O5: 0.00%, SiO2: 1.00%. And at 120 cycles we have a composition: FeO: 54.27% Cr2O3: 16.74%, NiO: 7.75% P2O5: 0.000%, SiO2: 1.67%.



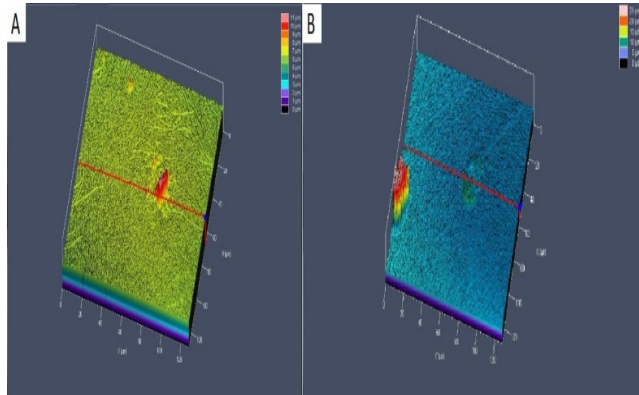
Source: Authors, 2016

Figure 5 EDS analysis tri-layer 10/70/20 A) 20 cycles B) 120 cycles

Is important to clarify that because low acceleration energies very used, were not achieved excite the K levels of many elements; plus some energies could be overlap, reporting elements that are not in the samples.

### C. Optical microscopy

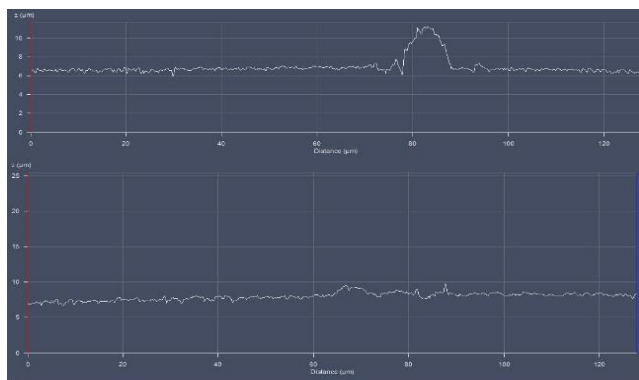
In Figure 6 the results for optical microscopy 3D, were realized in an optical microscope 3D brand ZEN 2009 LSM 700 with 100X magnification, we can observe that 20 cycles of heating for tri-layer 10/20/70 (Figure 6a) we have an average roughness of 0.185  $\mu\text{m}$ , and on the sample surface can be observed an almost uniform topology with few imperfections-topology (Figure 7, bottom).



Source: Authors, 2016

Figure 6 Confocal microscopy 3D, tri-layer 10/20/70 a) 20 cycles b) 120 cycles.

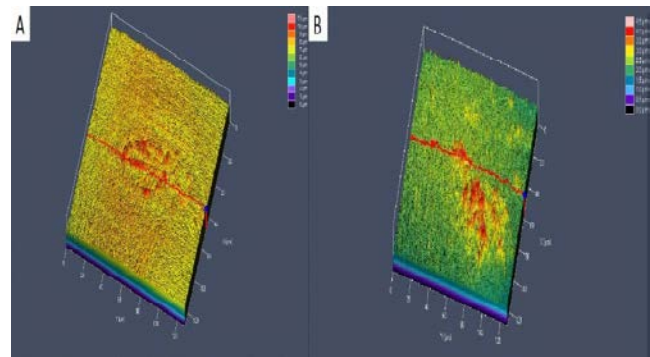
Observing confocal microscopy for the same sample 10/20/70 subjected to 120 cycles, we obtain a roughness of 0.595 microns (Figure 6b), while observing the imperfections on the sample have a size greater (Figure 7, top), suggesting that the coating shows signs of corrosion by generating an accumulation in specific areas of the surface.



Source: Authors, 2016

Figure 7 Confocal microscopy 3D, tri-layer 10/20/70 surface topology at 20 cycles (bottom) and at 120 cycles (top).

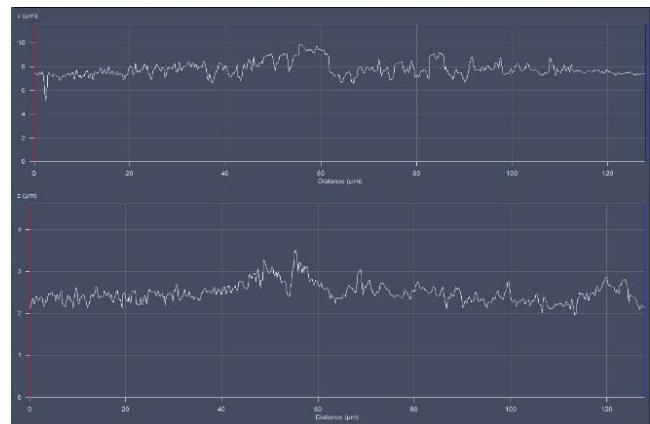
For the coating 10/70/20 at 20 cycles (Figure 8A) we can see a surface roughness of 0.312 microns, with small irregularities (Figure 9, bottom), suggesting that no formation of oxides on the surface and lesser degree that the sample 10/20/70 at 120 cycles



Source: Authors, 2016

Figure 8. Confocal microscopy 3D, tri-layer 10/70/20. A) 20 cycles B) 120 cycles.

For the coating at 120 cycles an average roughness of 0.228 microns (Figure 8B) was obtained, having a small variation with respect to the previous coating also it can be observed that oxide formation is not of great variation with respect to 20 cycles (Figure 9, top), which suggests this coating has a better behavior with respect to the composition 10/20/70.



Source: Authors, 2016

Figure 9. Confocal microscopy 3D, tri-layer 10/70/20 surface topology 20 cycles (bottom) and at 120 cycles (top)

Below is shown a table with results grouped for confocal microscopy test

**Table 1. Results of roughness by confocal microscopy**

COMPOSITION	PSa 20 cycles	PSa 120 cycles	Pa 20 cycles	Pa 120 cycles
10/20/70	0.185	0.595	0.476	0.421
10/70/20	0.312	0.228	0.491	0.177

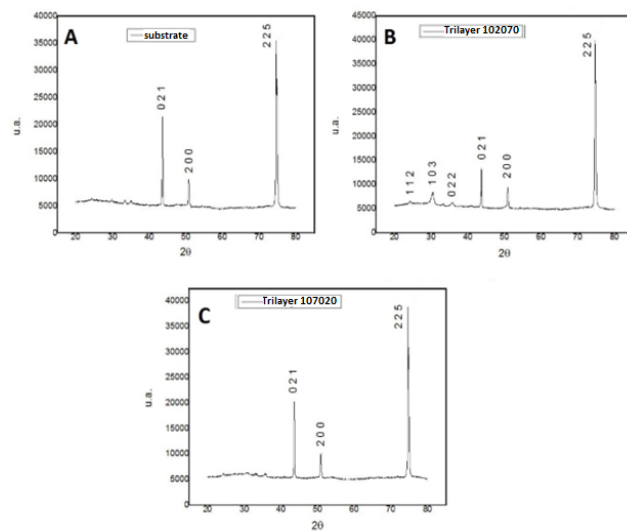
Source: Authors, 2016

### D. XRD analysis

According to the results of scanning electron microscopy where the apparent formation of a crystalline phase in the samples of composition 10/70/20 is observed, was carried out an analysis of

x-ray diffraction to confirm whether there was an ordered crystallographic structure. Once determined this phase, the stereographic planes corresponding to each peak and elemental composition were characterized, suggesting probable coating components. The main peaks were determined using the patterns from Crystallographic Act.

The analysis was carried out by performing a scan of 20 to 80 degrees, this means that the results are not only evidence of the surface composition, but also components in depth; that is, in the analysis was evaluated the chemical and structural composition of the coating and also most likely by intensity got to the base material, to evidence this was carried out the analysis for the base material without coating subjected to 20 and 120 cycles, which are shown in Figure 10A and 11A respectively.



Source: Authors, 2016

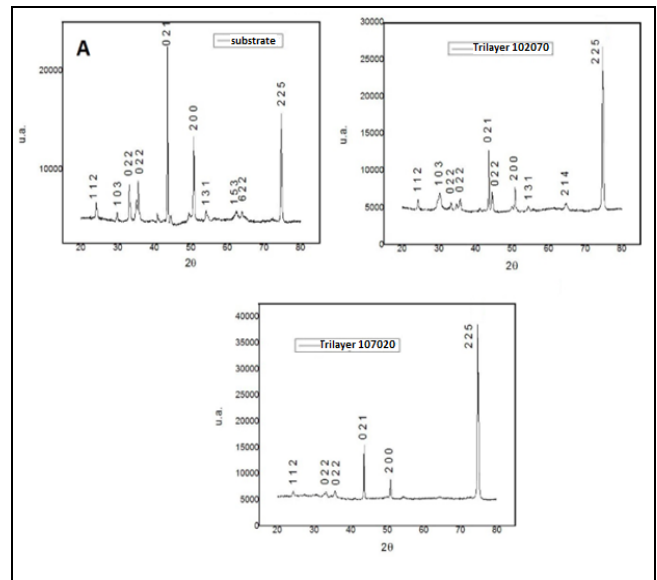
Figure 10. XRD results at 20 cycles A) Material without coating B) tri-layer 10/20/70 C) tri-layer 10/70/20.

In Figure 10B, we can see the characteristic peaks of the tri-layer 10/20/70 subjected to 20 cycles of heat treatment. The planes (1 1 2), (1 0 3), (0 2 2) correspond to the precursors of the coating, whereas the planes (0 2 1), (2 0 0) and (2 2 5) correspond to the base material.

Figure 11B shows the XRD diffractogram obtained for the tri-layer 10/20/70 subjected to 120 cycles of heat treatment, where in addition to the planes identified for the base material and coating, we can see the corrosion products in the planes (1 3 1) and (2 1 4).

Figure 10C shows the diffractogram for the tri-layer 10/70/20 after being subjected to 20 cycles of heat treatment, were found peaks corresponding to the base material by which it is considered that the coating is amorphous in nature and was not affected by treatment.

After being subjected to 120 cycles of thermal treatment, the coating of the tri-layer 10/70/20, shows characteristic peaks of the coating precursors (see Figure 11C).



Source: Authors, 2016

Figure 11. XRD results at 120 cycles A) Material without coating B) tri-layer 10/20/70 C) tri-layer 10/70/20.

#### IV. CONCLUSIONS

After being subjected to heat treatments, coatings compositions Si/Ti/Zr of the 10/20/70 and 10/70/20 respectively, showed differences in performance against corrosion and morphological changes. The coating tri-layer 10/70/20 showed better corrosion protection at high temperatures, less cracking and roughness changes. Therefore we can think about technological applications for this coating deposited by the sol-gel technique.

#### ACKNOWLEDGMENT

The authors thank the staff of the laboratories of Mechanical Engineering of the National University of Colombia who participated in conducting the tests of the materials used in this investigation. Likewise thank the Department of Physics, University Francisco de Paula Santander- San José de Cúcuta-Colombia for their collaboration in the development of this research.

#### REFERENCES

- [1] Chen, D., Jordan, E. H., Gell, M. and Ma, X. (2008). Dense TiO<sub>2</sub> Coating Using the Solution Precursor Plasma Spray Process. *J. of the Am. Ceramic Soc.* V.91(3), 865-872.
- [2] Krupa, A. N. D., Vimala, R. (2016). Evaluation of tetraethoxysilane (TEOS) sol-gel coatings, modified with green synthesized zinc oxide nanoparticles for combating microfouling. *Materials Science and Engineering C.*, 61, 728-735.
- [3] Wang, D. and Bierwagen, G. P. (2009). Sol-gel coatings on metals for corrosion protection. *Progress in Organic Coatings* 64, 327-338.
- [4] Adraider, Y., Pang, Y. X., Nabhani, F., Hodgson, S. N., Sharp, M.C. and Al-Waidh, A. (2013). Fabrication of zirconium oxide coatings on stainless steel by a combined laser/sol-gel technique. *Ceramics International*, 39, 9665-9670.

- [5] Yu, M., Liang, M., Liu, J., Li, S., Xue, B. and Zhao, H. (2016). Effect of chelating agent acetylacetone on corrosion protection properties of silane-zirconium sol-gel coatings. *Applied Surface Science* 363, 229–239.
- [6] Andrade, G.(2004). Sol-gel made Silicium-Zirconium and Silicium-Titanium covering conformation, (undergrade thesis). Cauca university., Cauca, Colombia.
- [7] Mafla, A.(2003). Silicium Titanium ceramic conformation by the sol-gel method., Cauca, Colombia.
- [8] Budd, KD., Dey, SK. and Payne, DA.(1985). Sol-gel processing of PbTiO<sub>3</sub>, PbZrO<sub>3</sub>, PZT, and PLZT thin films, *Br Ceram. Soc Pro*, 107-122
- [9] Lary, H. and Jhon, W.(1990). The Sol-Gel Process. *Chemical Reviews* 90(33), 33–72
- [10] Eduin, L.(2012). Tin dioxide 10% iron doped thin films synthesis and characterization., Medellin, Colombia.
- [11] Suzana, A.F., Ferreira, E. A., Benedetti, A. V., Carvalho, H. W. P., Santilli, C. V. and Pulcinelli, S. H. (2016 ). Corrosion protection of chromium-coated steel by hybrid sol-gel coatings. *Surface & Coatings Technology* 299, 71–80.
- [12] Francisco, O.(2007). High temperature evaluation of CVD-FBR deposited Al, Si and Al modified with Si and Hf coverings over Martensitic-ferritic steel (9-12% Cr), Madrid, España.
- [13] Mejia, A., Bautista, N. and Ortiz, C.(2011). SiO<sub>2</sub>-TiO<sub>2</sub>-ZrO<sub>2</sub> film elaboration by the sol-gel method. *Colombian Physics journal*, 11.

## AUTHORS

**First Author**–Karla Dayana Guerrero, Master Materials Science, Universidad Nacional de Bogotá, Colombia. E-mail:

[kdguerrerog@unal.edu.co](mailto:kdguerrerog@unal.edu.co).

**Second Author** – Erika Lorena Medina, Master Materials Science, Universidad Nacional de Bogotá, Colombia. E-mail:

[elmedinam@unal.edu.co](mailto:elmedinam@unal.edu.co).

**Third Author** –Néstor Giovanni

Yomayuzá, Mechanical Engineering, Universidad Nacional de Bogotá, Colombia. E-mail: [ngyomayuzas@unal.edu.co](mailto:ngyomayuzas@unal.edu.co)

**Fourth Author** –Jhon Jairo Olaya-Flórez, PhD.

Mechanical Engineering, Universidad Nacional de Bogotá, Colombia. E-mail: [jjolayaf@unal.edu.co](mailto:jjolayaf@unal.edu.co)

**Fifth Author**–Jorge Hernando Bautista-Ruiz, PhD.

Mechanical Engineering, Universidad Nacional de Bogotá, Colombia. E-mail: [jhbautistar@unal.edu.co](mailto:jhbautistar@unal.edu.co)

**Sixth Author**–Carlos Alberto Guerrero-Fajardo, PhD. Chemical Engineering and PhD. Chemistry, Universidad Nacional de Bogotá, Colombia. E-mail:

**Correspondence Author**– Carlos Alberto Guerrero-Fajardo, e-mail: [caguerrero@unal.edu.co](mailto:caguerrero@unal.edu.co), Cel. Pone: 057 3164308909.